Fracture Toughness Assessment of Poly(ethylene terephthalate) Blends with Glycidyl Methacrylate Modified Polyolefin Elastomer Using Essential Work of Fracture Method

D. E. MOUZAKIS,[1] N. PAPKE,[1] J. S. WU,[2] J. KARGER-KOCSIS[1]

[1] Institut für Verbundwerkstoffe GmbH, University of Kaiserslautern, PO Box 3049, D-67653 Kaiserslautern, Germany

[2] Department of Mechanical Engineering, Hong Kong University of Science and Technology, Clear Water Bay, Kowloon, Hong Kong

Received 18 August 1999; accepted 3 March 2000

ABSTRACT: The static fracture toughness of poly(ethylene terephthalate) (PET) melt blended with a modifier containing glycidyl methacrylate (GMA)-grafted ethylene-propylene rubber and homopolymerized GMA was studied on injection molded specimens by adopting the essential work of fracture (EWF) method. It was found that the essential and nonessential or plastic work both decrease with an increasing amount of modifier (up to 20 wt %) if the PET matrix is amorphous and nonaged. The scatter in the EWF data for the blend with 10 wt % modifier was found by presuming concurrent mechanisms between microcrystallization and morphology-dependent cavitation and fibrillation processes. © 2000 John Wiley & Sons, Inc. J Appl Polym Sci 79: 842–852, 2001

Key words: poly(ethylene terephthalate); blends; toughness; essential work of fracture; aging

INTRODUCTION

Nowadays soft drink bottles are preferentially produced of poly(ethylene terephthalate) (PET). This market success is mainly due to the transparency, thermal stability, chemical resistance, and beneficial barrier properties of PET. The widespread use of one-way PET bottles necessitates suitable alternatives for their recycling. Melt blending of PET with various polymers and elastomers offers a good opportunity to convert the recycled PET into high performance engineering plastics. However, this perspective has not been fully explored yet. Until now the common practice of toughening PET and other linear polyesters is the incorporation of core–shell type rubbers.[1] The advent of this approach is that the particle size of the modifier is well controlled. However, the recent trend is to replace these costly core–shell rubbers with low-cost functionalized rubbers and thermoplastics. The utilization of reclaimed PET and its blending with various polymers for toughness improvement was the aim of numerous works. PET blends with high density polyethylene and linear low density PE, which is functionalized by several techniques, was extensively studied.[2–4] Kwon and Chung[5] studied the mechanical behavior of rigid/rigid

Correspondence to: J. Karger-Kocsis (karger@ivw.uni-kl.de).

Contract grant sponsors: DAAD; HKUST, Hong Kong; Fonds der Chemischen Industrie (to J.K.-K.).

Contract grant sponsor: INCO-COPERNICUS, European Union; contract grant number: ERBIC15CT960706.

Journal of Applied Polymer Science, Vol. 79, 842–852 (2001)

PET/polycarbonate (PC) blends reinforced with an additional liquid crystalline polymer. Amorphous copolyesters were also employed in the past as a blend component for PET, and the results were interesting.[6] However, most worldwide efforts focused on the melt blending of virgin and recycled PET resins with various rubber types.[7–10] Rubbers seem to be the proper toughening agents for PET. Their addition results in improved toughness, provided that the rubber phase is finely dispersed in the PET matrix. This can only be achieved if the rubber is properly functionalized.

For linear polyesters the best results were obtained with various copolymers containing glycidyl methacrylate (GMA) units.[11–13] Because these copolymers are very expensive, suitable alternatives need to be found when PET recycling is targeted. An interesting option is to graft GMA on the rubber.[14] Grafting of GMA on polymers can be associated with the homopolymerization of GMA and thus with the formation of PGMA. The effect of the latter on the mechanical performance of PET blends has yet to be investigated. This article presents the results of studying the fracture behavior of PET blends with a GMA-grafted polyolefin rubber in the presence of PGMA.

EXPERIMENTAL

Materials and Methods

Materials

A commercial bottle grade PET (Kodapak 9921W, clear, number-average molecular weight = 26 kg/mol, weight-average molecular weight = 52 kg/mol, Eastman Chemical Co.) was used as the raw material for melt blending with the functionalized elastomer. Tafmer P 0480 (Mitsui Chemicals) was chosen as the elastomer for grafting and blending with PET. This thermoplastic elastomer is an ethylene-propylene rubber (EPR) and has a composition of about 80/20 wt % ethylene/propylene.

Elastomer Functionalization

GMA was grafted onto the EPR using a twin screw extruder (ZSK 25, Werner & Pfleiderer) equipped with a gravimetric feeding device for the polymer. The liquid GMA and liquid peroxide (Trigonox 29 B 90, Akzo Nobel) were fed into the molten EPR through the first degassing vent of an extruder via a peristaltic pump. The temperature of the separate extruder heating units was set to (from the hopper toward the die) 150, 150, 170, 170, 190, 190, 190, 170, and 150°C. The applied screw speed was 150 rpm. The dosage ratio for EPR:GMA:peroxide was fixed at 100:15:0.5. The functionalized EPR strand was subsequently granulated.

The amount of grafted PGMA was determined by applying the separation method of Al-Malaika.[15] The grafted EPR was first completely dissolved in boiling xylene. Adding a sevenfold excess of cold acetone to this solution precipitated the GMA-functionalized EPR whereas the residual monomeric GMA and PGMA remained in solution. The GMA content of the functionalized EPR was determined by Fourier transform IR spectroscopy using the calibration method of Papke and Karger-Kocsis.[14] Accordingly, the EPR contained 0.5 wt % grafted GMA and 8.9 wt % PGMA.

Melt Blending and Injection Molding

The mixing of PET and functionalized rubber (EPR-*g*-GMA + PGMA) was carried out at the Hong Kong University of Science and Technology, using a ZSK-30 twin screw extruder (Werner & Pfleiderer) equipped with an automatic feeder. The PET and EPR-*g*-GMA granules were dried in a vacuum oven for about 24 h before blending. The processing conditions and temperature gradients along the line of extrusion were set according to the recommendations of the PET manufacturer at a rotation speed of 105 rpm. The PET blends were quenched in a water bath and converted into granules by a rotating disk pelletizer. In this way, granules of three different blends were prepared: PET containing 5, 10, and 20 wt % in EPR-*g*-GMA + PGMA. All three types of blend pellets were again dried in a vacuum oven for about 24 h before injection molding. Dumbbell specimens for tensile tests and rectangular plates for the fracture toughness evaluation were injection molded at 270°C by a JM 88 MKIII-C (Chen Hsong Machinery Co. Ltd., Hong Kong) injection molding machine. The injection and cooling times were set at 6.0 and 3.5 s, respectively.

Blend Characterization

Thermomechanical Evaluation

The viscoelastic response of the toughened PET blends was studied by dynamic mechanical ther-

mal analysis (DMTA). An Eplexor™ 150 N (Gabo Qualimeter) DMTA machine was employed to carry out this test. Rectangular 60 × 10 × 1 mm (length × width × thickness) specimens of were cut from the dumbbells and were subjected to oscillating tensile loading consisting of a static preload (6 ± 0.2 N) on which a sinusoidal wave of 3 ± 0.1 N at 10 Hz frequency was superimposed. Heating occurred at a rate of 1 C°/min in a temperature range between −100 and 250°C.

Differential Scanning Calorimetry (DSC)

The melting behavior of the blends was studied by DSC in a DSC 821^e apparatus (Mettler Toledo). DSC traces were registered at a heating rate of 10°C/min on samples weighing about 10 mg. Samples were taken from the injection molded specimens, as well as from the extrusion melt blended pellets.

Blend Morphology

The dispersion and size of the particles of the functionalized elastomer were revealed by means of a scanning electron microscopy (SEM) instrument (Jeol 5400). Blend samples were annealed at 110°C for 8 h to facilitate the crystallization and thus to favor the brittle fracture of the PET matrix. Afterward, the annealed samples were fractured by an impact pendulum. The fracture surfaces of these samples were sputtered with a Pd/Pt alloy and examined with SEM.

Mechanical Properties and Fracture Toughness

Tensile Tests

Tensile tests under static testing conditions were carried out on a Zwick 1474 universal testing machine. The crosshead speed was set at 1 mm/min. The tensile yield strength and Young's modulus of the blends were determined using dumbbell specimens. A minimum of five specimens per blend was used to get the mean values.

Essential Work of Fracture (EWF)

The EWF was employed for the toughness assessment of the PET–rubber blends. According to the EWF theory,[16–18] a distinction is made between a process zone where the actual crack runs and a plastic zone that surrounds the process zone. Consequently, the total work required to fracture a precracked specimen can also be divided into two parts associated with each of the two zones mentioned above:

$$W_f = W_e + W_p \tag{1}$$

where W_f is the total fracture work, W_e is the work spent in the process zone, and W_p is the energy consumed in the plastic zone. The W_f can be determined by calculating the integral of force over displacement from the tensile tests performed on deeply double edge notched tensile specimens (DDEN-T) of varying ligaments. Because W_e is related to a 2-dimensional (2-D) plane it is therefore a function of area (lt) whereas W_p is dissipated in a 3-D plastic zone and can thus be considered a function of volume (l^2t), where t is the specimen thickness and l is the ligament. Equation (1) can also be expressed by the specific terms

$$w_f = w_e + \beta w_p l \tag{2}$$

where $w_f = W_f/lt$, $w_p = W_p/l^2t$, and β is a geometry factor associated with the shape of the plastic zone.

According to eq. (2), the work of fracture is a linear function of the ligament size. The w_e can be determined from the interception of the linear regression line, fitted to the w_f versus l graphs, with the y axis.[19] An important prerequisite of the EWF method is that the crack propagates only after the ligament is fully yielded. However, this requirement was not met for all the materials tested. A number of neat DDEN-T specimens of PET were stored at room temperature for approximately 9 months. They were also subjected to EWF testing in order to determine the extent of sensitivity of PET to aging.

DDEN-T 80 × 40 × 3 mm^3 (length × width × thickness, clamped length 50 mm) specimens were tested at a crosshead speed of 1 mm/min. The failure mode of the DDEN-T specimens was recorded in situ by IR thermography (IT).[20]

RESULTS AND DISCUSSION

Thermal Response

DMTA

DMTA spectra of the PET/modified EPR blends are presented in Figure 1. The complex E modulus (E^*), clearly shows a steep decrease at about 75°C, which marks the glass-transition tempera-

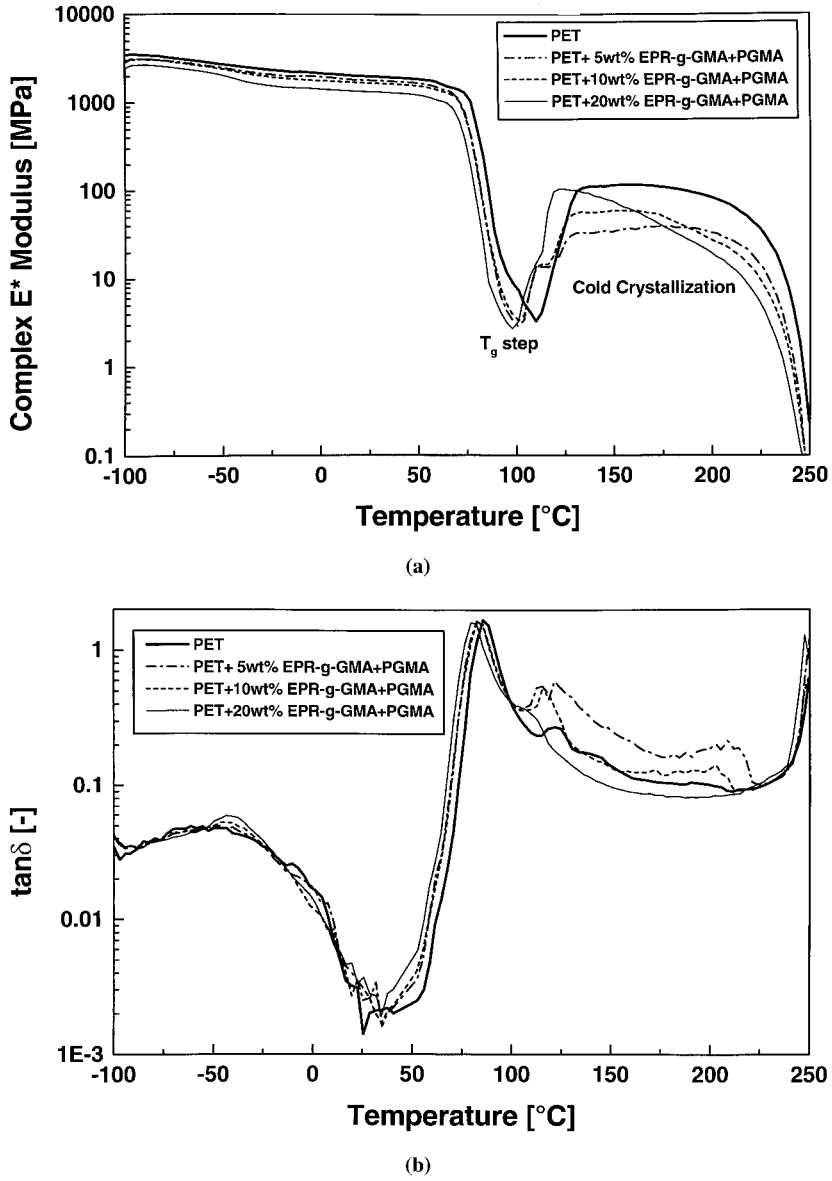

Figure 1 DMTA plots of the PET/EPR-*g*-GMA + PGMA blends: (a) the E^* modulus versus temperature and (b) the tan δ versus temperature.

ture (T_g) of the PET resin [Fig. 1(a)]. An interesting feature seen here is the shift in the T_g of PET toward lower temperatures with increasing elastomer content. This suggests some plasticizing effect of the functionalized EPR in the PET. The steep increase in E^* after the T_g step in Figure 1(a) evidences cold crystallization, suggesting that the injection molded specimens are essentially amorphous. This is due to the fast cooling during molding. A further shift in the onset of cold crystallization toward lower temperatures with an increasing rubber amount indicates that the EPR modifier nucleates the PET crystallization. Interestingly, there is practically no signal on the DMTA curves in Figure 1, indicating the existence of the EPR phase in the blends. Because EPR and PET are not miscible, one can suspect that the relaxation transitions of the EPR modifier are masked by the amorphous PET phase.

DSC

The DSC traces provide more information on the phase structure of the PET and its blends. Figure 2 shows the DSC traces of the injection molded blends. The small endotherm peak at 50°C is re-

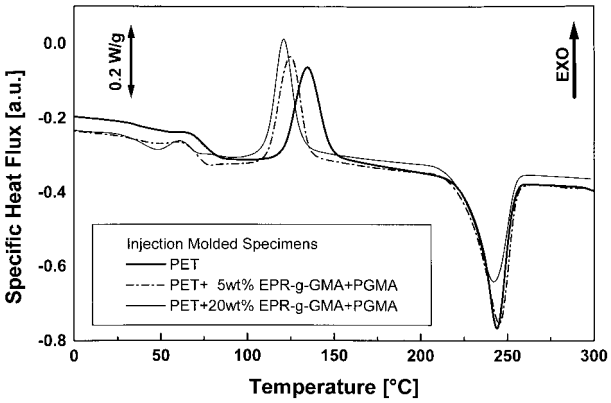

Figure 2 DSC scans on the injection-molded PET/EPR-*g*-GMA + PGMA specimens.

lated to the melting of the crystalline phase within the EPR whereas the peak at 250°C is due to the melting of PET. The exotherm peak at about 120°C is a result of cold crystallization. The nucleation effect of the EPR phase is again observed as the related peak with respect to this cold crystallization shifted toward lower temperature. The shift in the onset of the cold crystallization with the EPR content is in concert with the DMTA spectra [Fig. 1(a)]. The DSC behavior of the extruded blends, EPR-*g*-GMA + PGMA, and of the PET matrix can be seen in Figure 3. The T_g step of the PET can hardly be detected here. The melting peak at $T \approx 50$°C indicates that the EPR contains a crystallizable ethylene-copolymer fraction. The endothermic peak at about 150°C is of the annealing type caused by the extrusion blending conditions. Note that the melting range of PGMA also lies between 50 and 70°C and is thus masked by the melting of the EPR crystalline fraction.

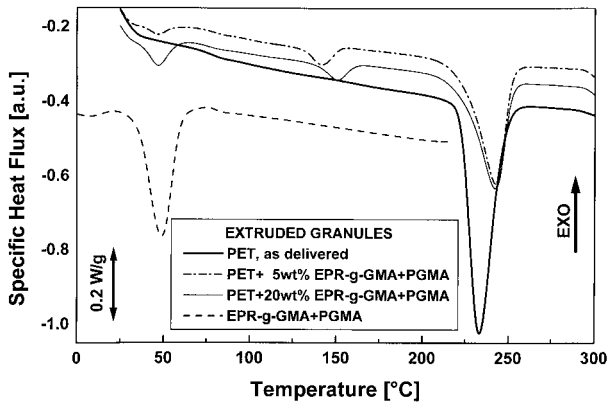

Figure 3 DSC scans on the blends consisting of PET and EPR-*g*-GMA + PGMA after extrusion compounding.

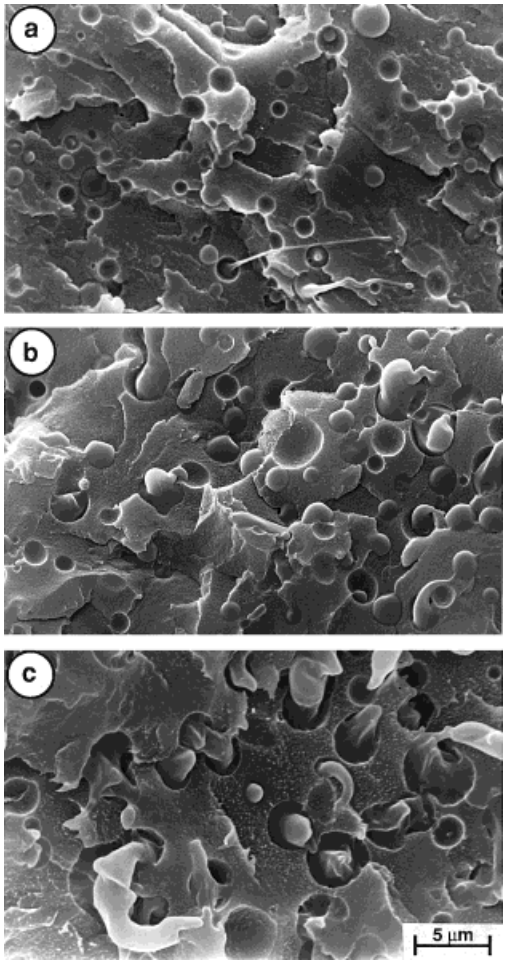

Figure 4 SEM pictures of the fracture surface of PET/EPR-*g*-GMA + PGMA blends showing the elastomer distribution: (a) PET + 5 wt % modified EPR, (b) PET + 10 wt % modified EPR, and (c) PET + 20 wt % modified EPR.

Blend Morphology

Figure 4 presents SEM photomicrographs of the three PET blends with various modifier contents. In all the pictures, elastomer particles or their empty nests in the PET matrix can be well resolved. The blend containing 5 wt % modifier shows the finest dispersion of all three blends with particle sizes below 3 μm [see Fig. 4(a)]. A slight increase in the spherical EPR particle size is observed in the blend with 10 wt % modifer [cf. Fig. 4(b)]. By contrast, the blend having 20% EPR-*g*-GMA + PGMA exhibits a coarser structure. On the fracture surface of the specimen, larger particles and particle agglomerates of more than 5 μm can be observed [Fig. 4(c)]. Recall that a mean particle size larger than 0.4 μm does not

Table I Tensile Mechanical Properties for PET/EPR-*g*-GMA + PGMA Blends

	E Modulus (GPa)	Yield Stress (MPa)	Yield Strain (%)
PET as molded	2.5	53.3	4.9
PET + 5 wt % mod. EPR	2.1	43.5	5.7
PET + 10 wt % mod. EPR	2.0	41.1	6.8
PET + 20 wt % mod. EPR	1.6	30.1	4.3

toughen the linear polyesters.[21] Accordingly, the microstructure of the blends indicates moderate toughness. This expectation is also supported by the poor interfacial adhesion between the PET matrix and the modifier particles (Fig. 4). Unfortunately, SEM did not help us to conclude where the PGMA is located. It can be presumed that PGMA works as a compatibilizer and is preferentially located in the interphase between the EPR-*g*-GMA rubber and PET.

Mechanical Properties

The *E* modulus and yield strength (σ_y) of the blends were both found to decrease with increasing elastomer content, which was expected (Table I). The blends with 5 and 10 wt % modifier possessed similar stiffness, which was slightly lower than that of the as-molded PET (Table I). On the other hand, the static mechanical properties of the blend with 20 wt % modifier were far less than those of the PET and its blends with less modifier. A similar effect was also observed for other systems like polypropylene/rubber/glass bead hybrid composites.[20] The results of the tensile tests suggested that the optimum amount of PET modification was likely around 10 wt %, where modulus and strength were kept at a reasonable high level and ductility, as expressed here by the yield strain, reached its maximum. Moreover, the yield strain (ϵ_y) of the blend with 20% EPR was lower than that of the PET matrix. This was probably due to the presence of the agglomerated elastomer phase, which reduced the stiffness and ductility.

The decline of the yield stress and Young's modulus were attributable to the softening effect of the modifying elastomer. An alternative explanation was based on the poor interfacial adhesion between the particles and matrix (Fig. 4). Because of the poor adhesion, the particles in the specimen were not load bearing and thus the actual load bearing area of the PET matrix became smaller with increasing elastomer content. This led to lower strength data.

Fracture Toughness

Stress–Strain Behavior of DDEN-T Specimens

Prior to discussing the EWF data, let us take a closer look at the stress–strain plots obtained of the DDEN-T specimens. In Figure 5 the apparent σ–ϵ plots of the DDEN-T specimens at a ligament of about 12 mm are collated for both neat and blended PET. The as-molded PET undergoes ductile fracture. Its ligament yields fully (sharp load drop after load maximum), followed by a stable crack propagation. An interesting change in the fracture behavior of the neat PET can be seen after 9 months of storage. After aging, brittle fracture occurs instead of ductile one, as seen in Figures 5 and 6. The change in the fracture response of the DDEN-T specimens after melt blending with the EPR modifier is also well resolved in Figure 5. It appears that the blends with 5 and 10 wt % EPR-*g*-GMA + PGMA modifier possess similar behavior. The process zones seen in Figure 6 are also very similar. Yielding can be clearly seen in these blends at a strain of about 2.0%, followed by stable necking and tearing until final fracture (Fig. 5).

The unstable fracture of the aged PET is shown in the macrophotographs taken of the fractured DDEN-T specimen halves in Figure 6. Observe the multiple cracking of the PET matrix toward the specimen bulk. This kind of cracking indicates that the material fractured under plane strain or at least under mixed plane stress and plane strain conditions. The DDEN-T specimens of the as-molded PET exhibit a typical ductile behavior,[20,22–24] which is displayed in Figures 5 and 6. Crack propagation is preceded by full ligament yielding (marked by the sharp load drop in the load trace in Fig. 5). The plastic zone of the related blend specimens in Figure 6 show stress whitening. This indicates that the energy dissipation mechanisms are likely matrix cavitation and crazing. Note that the whitened plastic zone in the DDEN-T specimen of the blend with 20 wt % EPR is the smallest. This corroborates our interpretation with respect to the static tensile results obtained on dumbbells (decrease of the net PET cross section due to large particles having poor adhesion to the matrix). It can thus be predicted that this blend will deliver the lowest toughness.

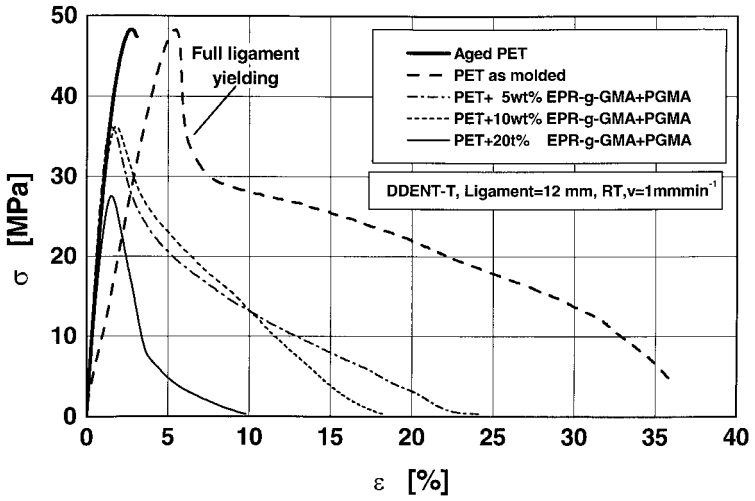

Figure 5 The typical apparent stress–strain (σ–ϵ) curves obtained for the DDEN-T specimens of PET blended with EPR-*g*-GMA + PGMA in various amounts.

IT

The failure sequence in the DDEN-T specimen of the as-molded PET is shown by characteristic IT frames in Figure 7. After the crack tip blunts [point A, Fig. 7(a)], the ligament yields instantaneously [point B, Fig. 7(a)]. The ligament yielding is accompanied by a local temperature rise of about 3°C [see cursor points in Fig. 7(b)]. The ligament yielding is followed by the formation of the plastic zone along with stable crack growth from both sides [points C and D, Fig. 7(a)]. The shape of the plastic zone can be approached by a shallow ellipse or diamond as also seen in Figure 6.

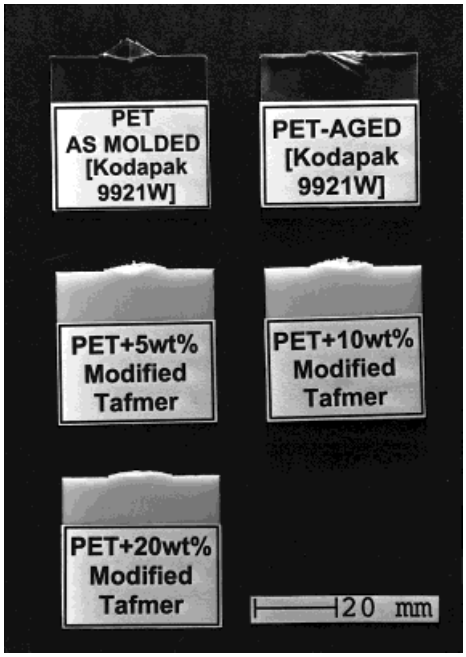

Figure 6 Macrophotographs of the fractured DDEN-T specimens of PET blended with EPR-*g*-GMA + PGMA in various amounts.

In the aged PET the above scenario changes substantially. The IT frame taken just in the moment of fracture shows some limited ductility of the specimen based on the heat map in the process zone (Fig. 8). This is in harmony with the small load drop observed prior to fracture in Figure 5. It implies that the EWF approach might still be used in this case. The IT response of the DDEN-T specimens with 10 wt % EPR-*g*-GMA + PGMA modifier blend showed some similarity to the as-molded PET, except that the ligament yielding was no longer a sudden process. Here the ligament yielding was accompanied by crack growth. Note that this behavior is common among polymers and polymer blends studied using the EWF concept.[17,18,25–27] This failure mode (i.e., yielding associated with crack growth) became even more pronounced for the blend with 20 wt % modifier. Accordingly, the energy dissipated in the post-maximum (postyield) range was reduced. This is a clear indication that the term βw_p in eq. (2) becomes negligible with increasing modifier content.

EWF

The variations of the specific work of fracture against the ligament length for the PET blends are presented in Figure 9. It can be seen that almost all materials exhibit a linear increase in the specific work of fracture with increasing liga-

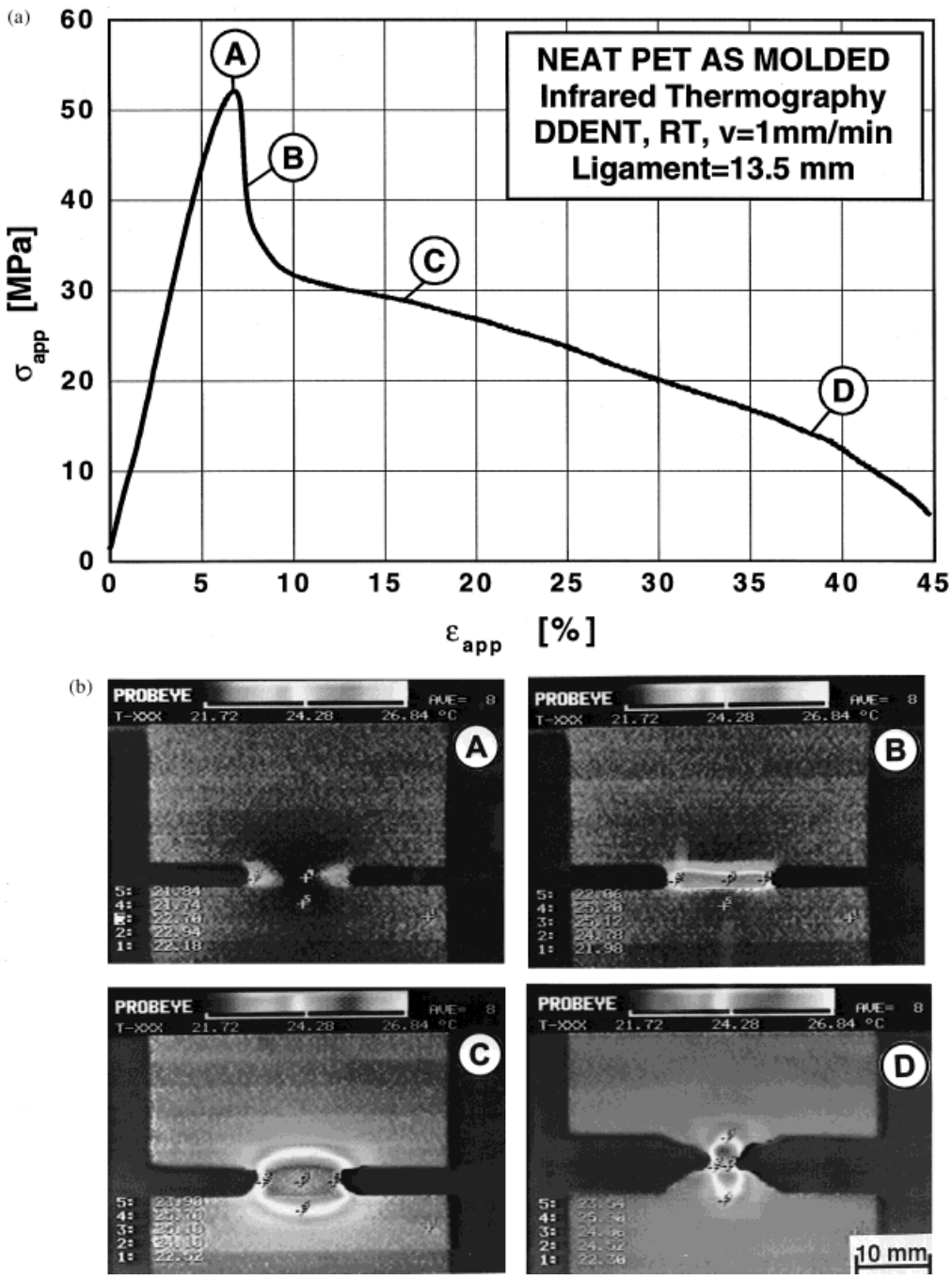

Figure 7 σ–ϵ curves (a) and related serial IT pictures (b) taken during testing of a neat, as-molded DDEN-T specimen of PET.

ment length, on which basis the w_e and βw_p terms were determined (see Table II). Our assumptions made in the previous paragraphs based on the mechanical properties, polymer blend morphology, and IT evaluation seem to be confirmed. The as-molded PET resin was characterized by a high toughness (i.e., the w_e and βw_p terms both had high values). After aging however, the PET exhibited a strong deterioration in both essential and plastic work data.

The increasing modifier (EPR-*g*-GMA + PGM) content resulted in a reduction in both the w_e and βw_p terms, except for the blend with 10 wt % modifier. An extremely high w_e and a very low

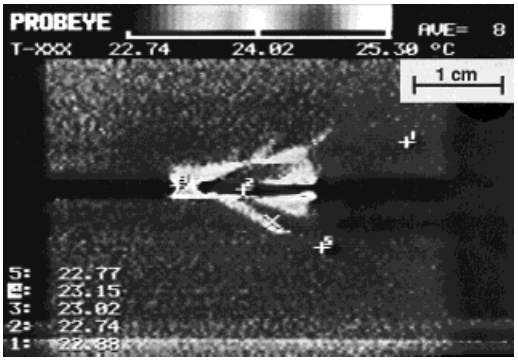

Figure 8 An IT frame taken at the moment of fracture of an aged DDEN-T specimen of PET.

βw_p was found for the blend with 10 wt % modifier. Karger-Kocsis[28] recently concluded that an increase in w_e is parallel with a decrease in the βw_p term. In other words, the critical crack initiation energy (or toughness, which is represented by w_e in this case) and the volumetric plastic work (βw_p, which is the actual energy dissipated in the plastic zone) cannot be improved at the same time. However, the authors stress that at this modifier amount (i.e., 10 wt %) the blends showed great sensitivity against the injection molding conditions. Efforts to model the effects of the injection molding conditions by annealing the molded parts were unsuccessful. All annealed specimens exhibited brittle failure and thus the EWF approach could not be adopted for them. Attempts to mold more specimens of the blends with 10 wt % EPR modifier and to reproduce their high toughness were not successful. Therefore, the results in Table II underlay a large scatter.

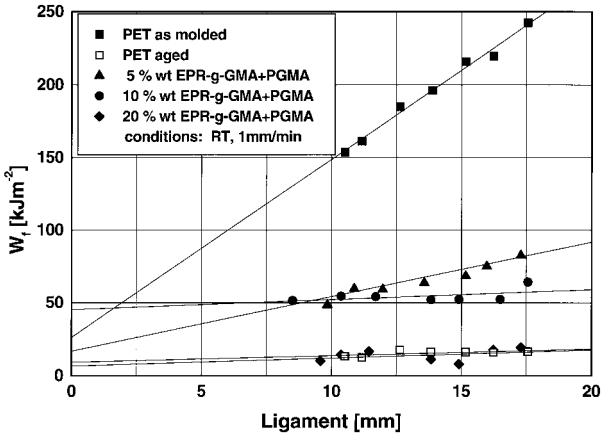

Figure 9 The specific work of fracture versus ligament plots for PET and PET blends.

Table II Essential Work of Fracture Data for PET/EPR-*g*-GMA + PGMA Blends

	w_e (kJ/m^2)	βw_p (MJ/m^3)	R
PET as molded	26.2	12.3	0.97
PET aged 9 months	9.2	0.44	0.91
PET + 5 wt % mod. EPR	16.8	3.74	0.90
PET + 10 wt % mod. EPR	13–45	0.68–2.90	0.87–0.83
PET + 20 wt % mod. EPR	6.6	0.54	0.85

This scatter is less prominent in respect to the related EWF plots (note that the correlation coefficients, βw_p, are quite high) but is reflected in the w_e and βw_p ranges given. The reason for this effect relies on the crystallization behavior of PET (see the related DSC and DMTA results). The superimposed effect of aging was pointed out earlier. The combined effect of crystallization and aging were likely responsible for the embrittlement of the PET blends. However, the major problem was related to the hardly reproducible crystallization of the PET matrix during molding and subsequent storage. This issue requires further in-depth investigation. Nevertheless, one could claim that aging negatively influences both the essential and nonessential (or plastic) work parameters. The results achieved on PET blends with 10 wt % EPR-*g*-GMA + PGMA confirmed the finding that the w_e (resistance to crack initiation) and βw_p (resistance to crack growth) changes are adverse to one another.[28]

Fractography

The as-molded PET failed by ductile tearing as Figure 10(a) shows. A very similar failure mode was also observed for amorphous copolyesters.[23] For the latter systems it was concluded that the w_e depends on the physical entanglement structure that also controls the formation of the plastic zone.[22] This analogy is fully acceptable if cold drawing took place instead of true plastic deformation. The onset of the latter can be substantiated by the IT frames (cf. Figs. 7 and 8), which demonstrate that the temperature in the ligament area never reached the T_g of PET. As a consequence, the deformation in the plastic zone occurred by cold drawing.

The embrittlement of the PET matrix due to aging is obvious in Figure 10(b). Ductile fracture

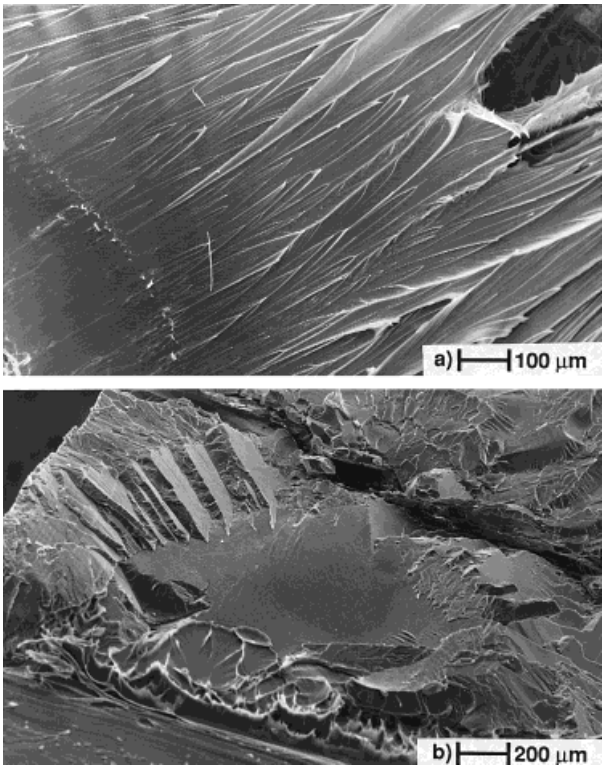

Figure 10 SEM microphotographs taken on the fracture surfaces of DDEN-T specimens: (a) as-molded PET and (b) aged PET.

can still be resolved in the vicinity of the notch region. Nevertheless, the overall fracture surface is of a brittle nature. Aging below the T_g may result in a microcrystalline structure as recently shown for PC,[29] because of which the polymer ductility is strongly reduced. Futher investigations are needed, however, to elucidate to which microstructural changes the observed embrittlement should be traced.

Figure 11 demonstrates that the functionalized EPR modifier causes matrix cavitation that in turn triggers crazing and matrix fibrillation. This failure mode was the same for all blends. The cavitation (voiding) process was responsible for the stress whitening observed in the plastic zones of the corresponding DDEN-T specimens. It was obvious that the fibrillation capability of the PET matrix depended on the matrix characteristics (microcrystallinity, entanglement), the mean interparticle distance of the modifier, and the particle–matrix interfacial adhesion.[30]

Coming back to the peculiar behavior of the PET blends with 10 wt % EPR modifier, one can trace it to the following mechanisms. A fine and uniform dispersion of the modifier favors the matrix cavitation and fibrillation. If this failure is not restricted to the fracture plane but extends into the bulk, the resistance to crack growth is enhanced. Consequently, the work dissipated in the plastic zone becomes larger. On the other hand, the modifier may act as a nucleator and induce the microcrystallization of the PET. The "morphological reinforcement" via microcrystallization obviously leads to higher w_e data (i.e., to an improvement in the resistance to crack initiation). At the same time, the stress transfer via the tie molecules is reduced. This decreases the resistance to crack growth (i.e., lowers the nonessential work of fracture data). The competition between them, which is also affected by aging, can be made responsible for the large scatter of the results found (see Table II).

CONCLUSIONS

Based on the above study conducted on blends of PET with modified EPR containing GMA-grafted rubber and PGMA, the following conclusions can be drawn:

1. High resistance to both crack initiation (specific EWF) and propagation (specific nonessential or plastic work) was found for nonaged, amorphous PET samples. This beneficial toughness response did not appear after aging.
2. The essential and apparent nonessential work of fracture both decreased with increasing modifier elastomer for all blends (up to 20 wt %). Deviation from this tendency was found for some blends contain-

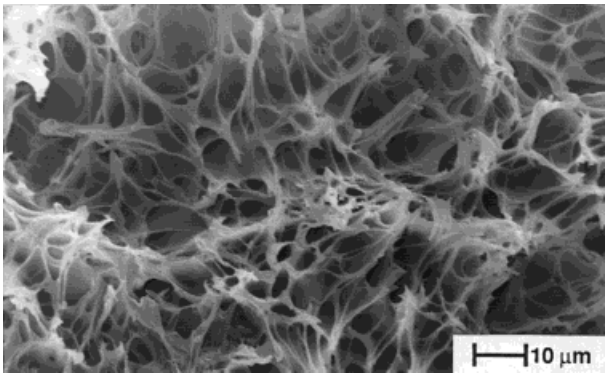

Figure 11 An SEM picture of the fibrillated and cavitated fracture surface of a PET blend (PET + 20 wt % functionalized EPR).

ing 10 wt % additive and exhibiting improved resistance to crack initiation. This behavior was however not reproducible and consequently the EWF parameters experienced a large scatter. This scenario was traced to the counteracting effects in favor of ductile (fine dispersion and small interparticle distance) and brittle (modifier-induced crystallization and physical aging) fractures.

REFERENCES

1. Keskkula, H.; Paul, D. R. In Rubber Toughened Engineering Plastics; Collyer, A. A., Ed.; Chapman & Hall: London, 1994; p 136.
2. Kalfoglou, N. K.; Skafidas, D. S.; Kallitsis, J. K.; Lambert, J.-C.; van der Stappen, L. Polymer 1995, 36, 4453.
3. Boutevin, B.; Lusinchi, J. M.; Pietrasanta, Y.; Robin, J. J. Polym Eng Sci 1996, 36, 879.
4. Márquez, L.; Sabino, M. A.; Rivero, I. A. Polym Bull 1998, 41, 191.
5. Kwon, S. K.; Chung, I. J. Polym Eng Sci 1995, 35, 1137.
6. Papadopoulou, C. P.; Kalfoglou, N. K. Polymer 1997, 38, 631.
7. Penco, M.; Pastorino, M. A.; Occhiello, E.; Garbassi, F.; Braglia, R.; Gianotta, G. J Appl Polym Sci 1995, 57, 329.
8. Kalfoglou, N. K.; Skafidas, D. S.; Kallitsis, J. K. Polymer 1996, 37, 3387.
9. Tanrattanakul, V.; Hiltner, A.; Baer, E.; Perkins, W. G.; Massey, F. L.; Moet, A. Polymer 1997, 38, 4117.
10. Abu-Isa, I. A.; Jaynes, C. B.; O'Gara, J. F. J Appl Polym Sci 1996, 59, 1957.
11. Hale, W.; Keskkula, H.; Paul, D. R. Polymer 1999, 40, 265.
12. Hale, W.; Keskkula, H.; Paul, D. R. Polymer 1999, 40, 3353.
13. Aoyama, T.; Carlos, A. J.; Saito, H.; Inoue, T. Polymer 1999, 40, 3657.
14. Papke, N.; Karger-Kocsis, J. J Appl Polym Sci 1999, 74, 2616.
15. Al-Malaika, S. personal communication, Budapest, December 1998.
16. Broberg, K. B. Mech Phys Solids 1975, 23, 215.
17. Mai, Y. W.; Cotterell, B. Int J Fracture 1986, 32, 105.
18. Yap, O. F.; Mai, Y. W.; Cotterell, B. J Mater Sci 1983, 18, 657.
19. European Structural Integrity Society, ESIS TC4 Task Group. Testing Protocol for Essential Work of Fracture; Les Diablerets: Switzerland, 1998.
20. Mouzakis, D. E.; Stricker, F.; Mülhaupt, R.; Karger-Kocsis, J. J Mater Sci 1998, 33, 2551.
21. Hourston, D. J.; Lane, S. In Rubber Toughened Engineering Plastics; Collyer, A. A., Ed.; Chapman & Hall: London, 1994; p 243.
22. Karger-Kocsis, J.; Czigány, T.; Moskala, E. J. Polymer 1998, 39, 3939.
23. Karger-Kocsis, J.; Czigány, T.; Moskala, E. J. Polymer 1997, 38, 4587.
24. Ferrer-Balas, D.; Maspoch, M. L.; Martinez, A. B.; Santana, O. O. Polym Bull 1999, 42, 101.
25. Levita, G.; Parisi, L.; McLoughlin, S. J Mater Sci 1996, 31, 1545.
26. Chan, W. Y. F.; Williams, J. G. Polymer 1994, 35, 1666.
27. Hashemi, S. Polym Eng Sci 1997, 37, 912.
28. Karger-Kocsis, J. J Macromol Sci Phys 1999, B38, 635.
29. Privalko, V. P.; Sukhorukov, D. J.; Karger-Kocsis, J.; Baltá Calleja, E. J. J Macromol Sci Phys 1999, B38, 27.
30. Michler, G. H. Kunstoff-Mikromechanik: Morphologie, Deformation und Bruchmechanismen; Hanser: München, 1992.